Diffusion and active transport in the cell. Simulations with Random Walkers. Entropy analysis

Pablo Lechón

May 29, 2019

Abstract

We present a review of two main processes that take place within the cells; diffusion and uniform directed flow)best exemplified by molecular motors). A review of some experiments regarding the measurement of diffusive dynamics is presented. Along with that, we do also review the anatomy of molecular motors and analyze some experiments that uncover their behavior in the cell. Finally, we provide to the reader with original work on simulations of both processes of diffusion and uniform directed flow with a system of pure or biased random walkers.
There are some final considerations about the entropy of this systems, and its time evolution.

1 Diffusion

One of the most important dynamical processes occurring within the cell is diffusion, the random oscillations of individual molecules in solution, also known as Brownian motion. When many cells are going through this process, the overall concentration can change giving place to ordered and directed movements of molecules down concentration gradients. This motion is only effective in short scale distances. The movement caused by diffusion is slow. The typical time it takes for a particle to diffuse a distance L is given by $t \approx L^2/D$, where D is the diffusion constant of the particle (it depends on the size of the particle, the temperature, and the viscosity of the surrounding fluid). Because diffusive motion is always present at molecular length scales, biological systems must tolerate, exploit, or inhibit Brownian motion in order to perform directed dynamic processes.

There are several ways to identify and measure diffusive dynamics inside the cell. In this review, we summarize some of them.
Fluorescence Recovery After Photobleaching (FRAP) denotes a method for measuring two-dimensional lateral mobility of fluorescent particles. A small spot on the fluorescent surface is photobleached by a brief exposure to an intense focused laser beam. The recovery of the fluorescence is due to the replenishment of intact fluorophore in the bleached spot by lateral transport of the surrounding surface. This method provides valuable knowledge on the diffusion dynamics of the cell, namely; (a) identification of transport process type (either a random diffusion or uniform directed flow), (b) determination of the absolute mobility co-

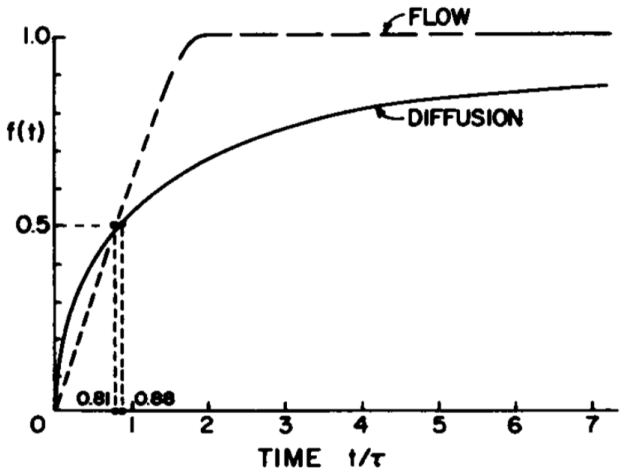

Figure 1: Fractional fluorescence recovery $f_K(t)$ vs t/τ for diffusion flow with a uniform circular disc laser beam.

efficient (either the diffusion constant or the flow velocity) and (c) the fraction of total fluorophore which is mobile. D. Axelrod et. al, 1976, provide a tutorial on this experimental method by analyzing a case of some model experiments on aqueous solutions of rhodamine 6G. By fitting experimental data to the theoretical curves in 1 we can obtain the nature of the transport (diffusion or directed flow), the relative proportion of mobile vs immobile fluorophore in the sample (which may be of considerable interest in mobility measurements on living cells), and the apparent diffusion constant D or flow rate V. Absolute determination of D and V depend upon determinations of beam size and profile. Specifically, we can obtain these coefficients with the following formulas:

$$D = \frac{w^2 \gamma_D}{4\tau_{1/2}} \tag{1}$$

$$V = \frac{w^2 \gamma_F}{4\tau_{1/2}} \tag{2}$$

Constants γ_D and γ_F depend, in general, upon beam shape, type of transport and the amount of bleaching-induced in a certain amount of time. For circular beams, like is the case in the figure, these coefficients don't depend on the amount of bleaching. $\tau_{1/2}$ is the time for which $f_K(\tau_{1/2}) = 1/2$
We can appreciate in figure 1, where the fractional fluorescence recovery vs t/τ has been plotted, how the recovery time for the diffusion process follows a square root form. On the other hand, the directed flow goes as a straight line. This makes sense, because, the rhythm of recovery is constant for an unidirectional flow. This curves of course, are only defined for $f_K(t) < 1$. After that, the fluorescence reaches the pre-bleach value (normalized to 1 in the plot).

Fluorescence Correlation Spectroscopy (FCS) is another method in which temporal fluctuations of the fluorescence intensity in a small region of the cell is analyzed through the use of time-dependent correlation functions. Diffusion constant and other characteristics of the molecular motion can be uncovered with this method. The third and oldest method is by monitoring diffusive dynamics through explicit particle tracking.

2 Molecular Motors

Merely diffusion is not sufficient to explain directed movements, such as muscle contraction. A directed flow demands mechanisms that convert chemical energy (usually by consumption of ATP, which stands for adenosine triphosphate) into mechanical energy. Molecular motors are key tools used by the cell to perform active transport and maintain the non-equilibrium conditions necessary within the cell.
The different kind of motors can be grouped

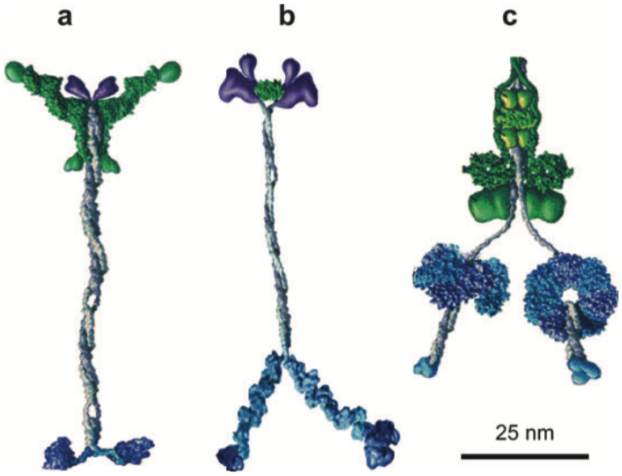

Figure 2: Domain structures of (a) conventional kinesin, (b) myosin V, and (c) cytoplasmic dynein. The tail domains are at the top, and the motor domains or heads are at the bottom. The (approximate) scale bar indicates 25 nm.

into 4 main subcategories: Translational motors, Rotary motors, Polymerization motors, and Translocation motors. In this review, the focus is going to be in translational motors.
Processive motor proteins, such as kinesin, dynein, and certain myosins, step unidirectionally along linear tracks (microtubules and actin filaments) and play a crucial role in cellular transport processes, organization, and function. For these motors, the most crucial parts are the motor domains, often called "heads", where the enzymatic activity takes place and which bind strongly to specific molecular tracks, such as microtubules and actin filaments. As seen in figure 2 (domain structures), the motor domains are connected by coiled-coil structures to tail domains that also play a role in the activity of the motor. These connect to cellular cargo, such as vesicles and organelles, and in the absence of a suitable load, the tail domains may bind to the motor domains and thereby cut off the enzymatic activity. Several classes of motor proteins function as single independent entities as does a locomotive: they move on their tracks by repeatedly hydrolyzing ATP molecules (at rates of order one per 10 ms), taking hundreds of discrete, close-to-equisized, nanoscale steps before finally dissociating. Among such processive motor proteins are conventional kinesin, cytoplasmic dynein, and myosins V and VI. The first pair walk on microtubules, kinesin towards the plus (or fast-growing) end, whereas dynein is minus-end directed.
The most informative data concerning the dynamics of motor proteins have recently come from single-molecule experiments, which include optical-trap spectrometry, magnetic tweezers, Forster resonance energy transfer (FRET), dynamic force microscopy, fluorescent imaging, and many other techniques. The ability to passively monitor and actively influence the dynamics of individual single molecules (in particular by imposing forces and torques) provides a powerful tool for uncovering motor mechanisms. One of the most successful and widely used methods is optical-trap spectrometry. In this approach, a single motor protein is chemically attached to a micron-sized or smaller bead that is captured by an external laser beam. The bead follows the motion of the motor molecule as it binds to its track and proceeds to move, as it can be seen in figure 3.

Figure 4(optical-trap measurements), shows the striking results of such a force-displacement-time experiment for kinesin moving on a microtubule. Immediately, in the presence of ample ATP (typically at millimolar levels), the motor starts to drag the bead out of the trap not continuously but rather by taking a series of plus-end-directed discrete steps. The step length, d, proves close to 8.2 nm which is the periodicity of a

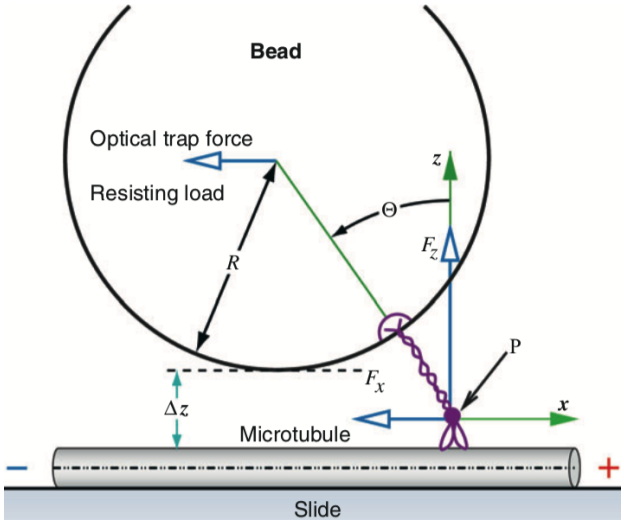

Figure 3: diagram of a kinesin/microtubule/bead complex in an optical-trap experiment. The microtubule is fixed to a glass slide that can be moved relative to the (fixed) optical trap. The force Fx exerted on the bead by the optical trap is transmitted by the tether to the point of attachment P on the motor at which the two heads are joined

microtubule protofilament.
When the bead is drawn further out of the trap, the resisting force (F_x in figure 3) increases and the motor slows down, reaching stall conditions (i.e., a zero mean velocity, V) at loads of 7 to 8 pN. As evident in figure 4 (optical trap measurements), reverse or back steps may then occur until, after some time, the motor detaches from the track (at t ≈ 6.3 s)

3 Random Walkers

In this review, we examine two powerful roles for random walk models, namely, as the basis for considering the problem of diffusion, and as a scheme for characterizing molecular motor dynamics.

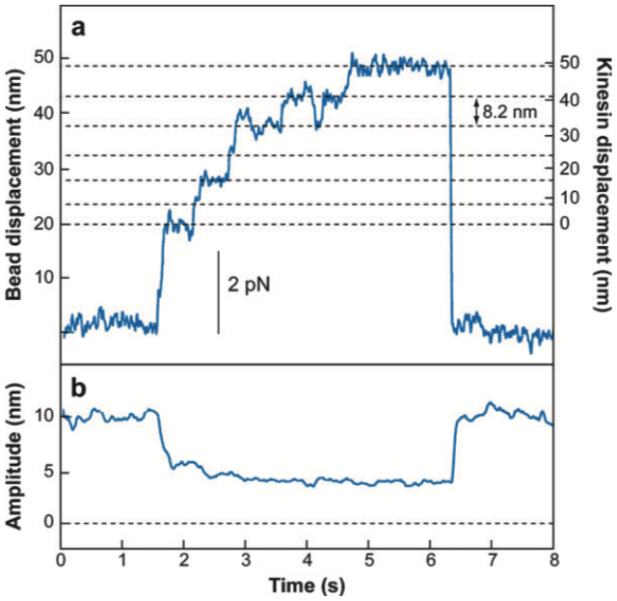

Figure 4: Optical-trap measurements of the motion of a single kinesin molecule at 20 μM ATP. (a) Bead displacement as a function of time. (b) Measurements of time-dependent kinesin-to-bead stiffness.

We are first going to tackle the problem of diffusion with a model of random walkers in 1D.
From Fick's Law and Conservation of Mass, one can derive the diffusion equation;

$$\frac{\partial c}{\partial t} = D\frac{\partial^2 c}{\partial x^2} \tag{3}$$

The solution to this equation will depend of course on the initial and boundary conditions. One of the most useful tools corresponds to knowing how to solve this equation for a spike of concentration at the origin at time t = 0. In particular, if at time t = 0 we start with N molecules (random walkers) in an infinitesimally small region around x = x_0, the concentration profile will evolve in the following way:

$$c(x,t) = \frac{N}{\sqrt{4\pi Dt}}\, e^{-x^2/4Dt} \tag{4}$$

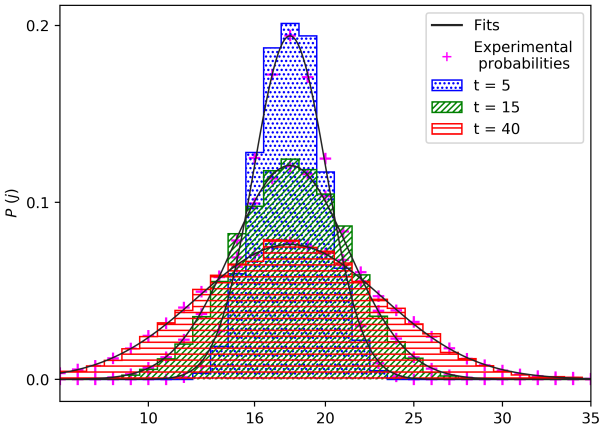

Figure 5: Probability distributions for a specific time. The fit of the Green's equation to the experimental data have been carried out, yielding a value for the diffusion constant D = 0.37. This value has been obtained averaging the three values from each of the fits, because, D doesn't depend on the time.

Further, by dividing by N, this equation can then be interpreted as giving the probability density for finding a particle between x and x + dx.

$$p(x,t) = \frac{1}{\sqrt{4\pi Dt}}\, e^{-x^2/4Dt} \qquad (5)$$

The solution above is often denoted as the Green's function of the diffusion equation. The profile has the form of a Gaussian of width $\sqrt{2Dt}$ and hence it increases as the square root of the time. Note that for this case, the mean position of the concentration distribution does not change with time. This corresponds to the absence of a drift term.

An attempt to computationally simulate the problem of diffusion within the cell was made using python. We created a grid of 32 slots and set N = 8000 random walkers at position 16. In this case, the random walkers are non-biased. This means that the probability that they go to the right left or stay put, is the same. In figure 5 we can appreciate three elements. First, the histogram of our results at different times, thus, the number of random walkers at each position after a specific number of iterations of the program normalized to the total number of random walkers. Second, the probability to find a random walker at position j after a specific number of iterations (magenta crosses). Note that these two things are conceptually different, though, they should be numerically fairly similar. The probability to find a random walker at position j at time t has been calculated experimentally from the number of random walkers at positions j, j+1, and j-1, whereas the histogram is just the number of random walkers at position j and time t. The magenta crosses (ie., the experimental probability) should by definition be closer to the theoretical value of the probability calculated from the Green's function of the diffusion equation. Finally, the fit of this last equation to the probabilities is the black line. Green's equation has D as a free parameter, so the fit provided us with the value of the diffusion coefficient in arbitrary units.

Translational molecular motors can also be thought of as random walkers. The basic idea is to consider the range of possible conformational states of a motor. One of the ways we will describe motor dynamics is that of a translational motor moving along some periodic track such as an actin filament or a microtubule. This class of models imagines n slots along the track that are each the same. Within each of these slots, the motor can be in any one of the P distinct states. That is, motors are characterized by a state space in which the motor can occupy a set of geometric positions, and at each such position, it can occupy a set of internal structural states. This perspective doesn't apply to a simple translational motor such as kinesin, where the geometric positions correspond to different posi-

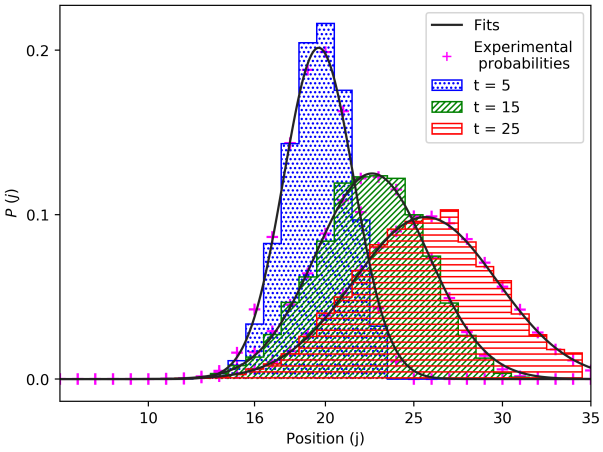

Figure 6: For this case, the diffusion averaged diffusion constant was D = 0.35 and averaged mean velocity was V = 0.31. In this case, the fitted equation had two free parameters that were determined.

tions of the motor molecule along the microtubule, and the internal state refers to both conformational states of the motor as well as its binding to other molecules such as ATP. The simplifying assumption that the motor position along the track can be discretized into equal-sized boxes is a reflection of the observation that real motors generally move in quantized steps of a characteristic size, like the motor in figure 4 (optical trap measurements). The most simple example is now considered, the one-state model. We assume that the motor has no internal states and simply hops from one site to the next with forward rate $k_+(F)$ and a backward rate $k_-(F)$ under the action of the force F. Therefore, the probability per unit time of the motor moving forward by one site is $k_+(F)$, and backward is $k_-(F)$. The treatment that is about to be made cannot be applied to any real motor, because motors must couple energy utilization (for example, in form of ATP hydrolysis) to a mechanical conformational change, indicating that there must be at least two states that we would have to account for. An expression of an evolution equation for the probability distribution of the motor $p(n,t)$, that is, the probability that we have a random walker at position n at time t, can be derived after some math, arriving at the equation

$$\frac{\partial p}{\partial t} = -V\frac{\partial p}{\partial x} + D\frac{\partial^2 p}{\partial x^2} \tag{6}$$

where we have made the definitions

$$V = a\left[k_+(F) - k_-(F)\right] \tag{7}$$

and

$$D = \frac{a^2}{2}\left[k_+(F) + k_-(F)\right] \tag{8}$$

where a is the length of each unit in the microtubule.

This is the equation for diffusion in the presence of a drift term. The probability distribution p(x,t) (x is the equivalent variable to the variable n, in a continuum space) describing a one-state motor can be characterized by equation 6, which is a biased diffusion equation. Also known as the Smoluchowski equation. The physical essence of this equation is that motors move with an average velocity V. However, if we start a collection of motors on parallel filaments all at the same time we will find that, over time, they spread out in a way characterized by the diffusion constant D. To see this explicitly we can solve the equation analytically, arriving at the following solution

$$p(x,t) = \frac{1}{\sqrt{4\pi Dt}} e^{-(x-Vt)^2/4Dt} \tag{9}$$

This equation is basically a Gaussian equation which means travels throughout the grid at an average velocity V and diffuses over time with a diffusion constant D.

Again, this system was computationally simulated with python. The considerations

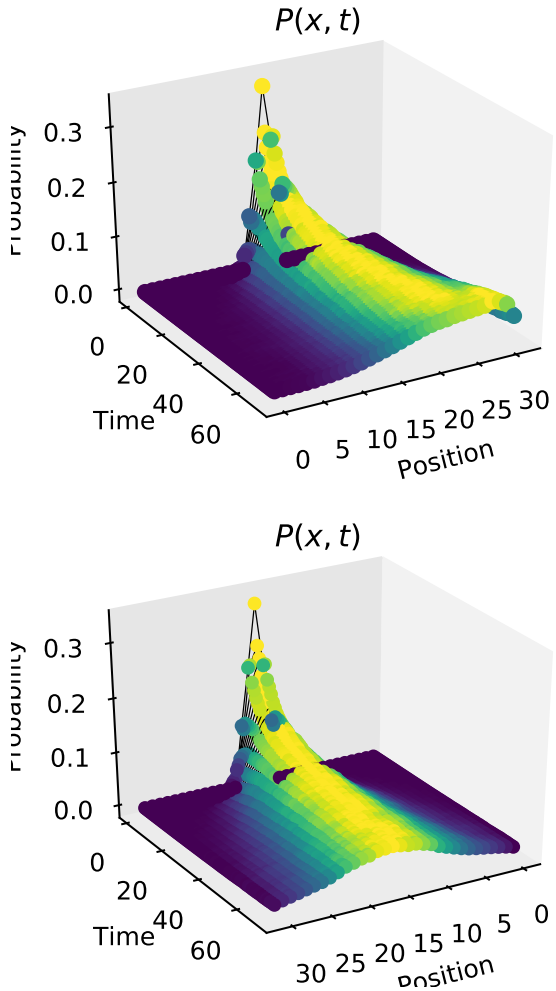

Figure 7: Probability distributions obtain for a set of N = 8000 random walkers over a grid of L = 31 pints.

made were the same as for the diffusion case, with the only difference that now we have different probabilities. In this particular case, we chose the probabilities to be $p_r = 0.3$, $p_c = 0.5$, and $p_l = 0.2$. As a result from this heterogeneus probabilities, we have generated a biased random walker. This simple model represents a molecular motor aproximated to zero order.

Finally, we include also a 3D plot with the evolution of the system of random walkers for both cases (the biased and non-biased case). In this case, we have represented 71 iterations of the program, enough to appreciate the diffusion and the directed movement of the random walkers.

4 Entropy

One of the big questions entailing biophysics is the fact that any process that occurs will tend to minimize the free energy and maximize the entropy. This is why the entropy is a crucial concept in biophysics.
That is the reason why we study the entropy of both of the systems we have proposed to simulate diffusion and directed motion.
Entropy has always been thought of the number of microstates in a system. However, it can also be thought from a theory of the information point of view. The key fact is that the less information we have, the bigger the entropy becomes.
This property is well captured in the probabilistic entropy expression that Boltzmann proposed in the 19th century.

$$H = -\sum_{i=1}^{N} p_i \log p_i \tag{10}$$

For example, for a two state system, with states A_1 and A_2, and probabilities $p_1 = p$ and $p_2 = 1 - p$. The above formula would yield an entropy as a funciton of the probability p

$$S(p) = -\left[p \ \log p + (1-p) \ \log(1-p)\right] \tag{11}$$

This function of p has its maximum at $p = 0.5$. This makes sense if we have in mind the idea of entropy as a lack of information. If the probabilities $p_1 = p_2$, we have less information than if $p_1 > p_2$, and therefore, the entropy associated to a system of equiprobable states, should be higher than

that associated to a system with predilections for some states.

In our simulation with python, we calculated the entropy after every iteration. Since we obtained an experimental probability for a random walker to be at position j at time t, we can use that probability to compute the entropy of the whole system at time t in agreement with equation 10.
If we do this for every iteration on the computations, we obtain the time evolution of the entropy for both systems. This is represented in figure 8 (entropy evolution)
As it was already discussed it is expected

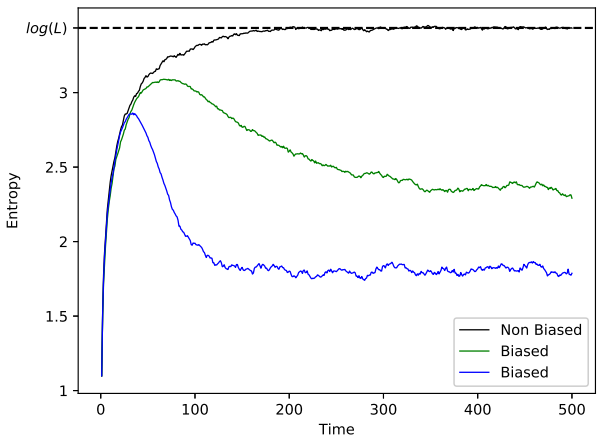

Figure 8: Time evolution of the entropy. The oscillations around the final entropy are due to the finite size of our system. The level of bias of the blue curve is higher thatn that of the green curve.

that the entropy of the biased random walkers system ends up being lower than the one associated with the non-biased system because we have more information of the first system, ie. we have some states (positions in the grid) that are more likely to happen. In our simulated case, these states are the ones to the very right of the grid. For the non-biased random walker, a prediction of the final entropy can be made. This is because we know the final distribution of the configuration. It will be a uniform distribution. Therefore, at $t = \infty$ we have that

$$H(\infty) = -\sum_{i=1}^{L} p_\infty(j) \log p_\infty(j)$$
$$= -\sum_{i=1}^{L} \frac{N}{L} \log\left(\frac{L}{N}\right) = \log(L)$$

However, things are slightly different for the biased random walkers. In this case, the final distribution is not a uniform one. Thus, the entropy will be lower, as it can be seen. This is due to the finite size of the system. In figure 8 (entropy evolution) we can appreciate how the entropy curves of the biased random walkers start being exactly the same as the non-biased curve. At the very beginning, the random walkers don't see the boundaries of the system, and therefore, they evolve to a uniform distribution too. The only difference would be that the uniform distribution would move across the grid.
Due to the finite size of our grid, the random walkers soon reach the limit, and they can't keep diffusing. Therefore they don't form a uniform probability distribution, and their final entropy is lower. Two curves associated with the biased random walkers system have been plotted in the figure. The green curve is a less biased curve. The random walkers take longer to reach the wall of the grid, and therefore they stick to the non-biased curve for a longer time.

5 Further work

Simulations on non-biased random walkers are key to understand diffusive processes within the molecule. ADN entails a good example of why messuring diffusion constants is

important in cell biology. The diffusion constant is related to the polymer size R by the Einstein relation

$$D = k_B T / 6\pi\eta R$$

However, our treatment has been a rather modest attempt to modelize the problem. First of all, we have simulated a 1D random walker. Also, we have allowed positions to be occupied by more than one walker. This is equivalent to simulate a dilute-solution enviroment. However, diffusion in crowded enviroments, such as within living cells, is more subtle than that. The constrain we would have to impose in order to simulate a crowded enviroment would be that no more than one random walker can occupie the same position in the grid. As a result, we would have that

$$p_r = p_l = \frac{1}{2}(1 - \phi)$$

where ϕ is the probability that a chosen site is occupied by a molecule. Theoretical results yield that in this case, the diffusion constant would be

$$D = D_0(1 - \phi)$$

where D_0 is the diffusion constant of a random walker wen no other molecules are present. We can see how diffusion in a crowded enviroment would be significantly slower that the one we have simulated.

Furthermore, simulations on biased random walkers are also a great tool to understand molecular motors. In this review, we have ignored the possible internal states that the motor can have. We have only consider that a full description of a particular motor at any instant in time can be determined by its position within the filament. However, we could have introduced another random index, that specifies the internal state. This description would have been more complete. An interesting experiment to carry out would be to perform multiple simulations with this better description of the biased random walker for different levels of biases. This would provide us with a set of diffusion coefficients and average velocities, which can be measured experimentally. From this data one could potentially determin kinetic rate constants.

Finally, there are some considerations regarding the study of entropy that I would have like to adress. A study of the dependence of the asymptotic value of the entropy on the size of the grid for differently biased systems could have been carried out if there was more time. I would have also studied the dependence of this same value on the level of bias. Maybe there is a way to predict this value based on the asymptotic probability distribution. If there was a way to analytically obtain this expression, we could have performed a calculation similar to that one done for the non-biased system.

Overall, I have enjoyed much spending nights in my bed, programming and getting those beautiful plots done as well as reading articles that provide a background to my work.

References

[1] Anatoly B. Kolomeisky and Michael E. Fisher
Molecular Motors: A Theorist Perspective

[2] Axelrod D, Koppel DE, Schlessinger J, Elson E, Webb WW.
Mobility measurement by analysis of fluorescence photobleaching recovery kinetics.

[3] Phillips R, Kondev J, Theriot J, Garcia GH, Orme N.
Physical Biology of the Cell

[4] LaTeX
`www.latex-project.org`

[5] Python

`http://www.python.org/`